In-depth investigation of EPR spectra of Mn^{2+} ions in ZnS single crystals with pure cubic structure

2009 J. Phys.: Condens. Matter 21 145408

(http://iopscience.iop.org/0953-8984/21/14/145408)

J. Phys.: Condens. Matter **21** (2009) 145408 (7pp) doi:10.1088/0953-8984/21/14/145408

In-depth investigation of EPR spectra of Mn^{2+} ions in ZnS single crystals with pure cubic structure

S V Nistor and M Stefan

National Institute for Materials Physics, POB MG-7, Magurele-Ilfov, 077125, Romania

E-mail: snistor@infim.ro and mstefan@infim.ro

Received 19 December 2008, in final form 29 January 2009
Published 13 March 2009
Online at stacks.iop.org/JPhysCM/21/145408

Abstract

The X (9.8 GHz)-band electron paramagnetic resonance (EPR) properties of substitutional Mn^{2+} ions in high quality cubic ZnS single crystals grown from $PbCl_2$ flux have been thoroughly investigated. Accurate spin Hamiltonian (SH) parameters: $g = 2.002\,25 \pm 0.000\,06$; $a = (7.987 \pm 0.008) \times 10^{-4}$ cm^{-1} and $A = -(63.88 \pm 0.02) \times 10^{-4}$ cm^{-1} were obtained by simulation and fitting to the experimentally allowed transitions recorded for the magnetic field aligned within $\pm 0.25°$ along the main crystal axes. The normally forbidden hyperfine $M = +1/2 \leftrightarrow -1/2$, $\Delta m = \pm 1$ transitions were also observed. Their position was found to be in agreement, within the experimental accuracy of $\Delta H = \pm 0.01$ mT, with calculations using the same SH parameters. The angular variation of the ratios of the intensities of the central forbidden to the allowed transitions could be accounted for only by including an additional constant contribution. The observed line broadening of the $M = \pm 1/2 \leftrightarrow \pm 3/2$ and $\pm 3/2 \leftrightarrow \pm 5/2$ fine structure transitions and their line width variation in a (110) plane have been quantitatively described by considering a random distribution of lattice strains at the Mn^{2+} impurity ions. The influence of the forbidden transitions and line broadening on the EPR spectra line shape of the Mn^{2+} ions in cubic ZnS crystalline powders is also examined.

1. Introduction

Zinc sulfide is one of the best known II–VI compound semiconductors, which has been extensively investigated due to its outstanding physical properties, in particular its light emission ranging from red to blue, depending on the kind of impurities it contains [1]. Transition metal ions ($3d^n$, $4f^n$) are the most interesting impurities as they introduce deep levels in the gap region, which can influence not only the optical, but also the electrical and magnetic properties [2, 3]. There is now a revived interest in basic research on ZnS crystals containing transition ions, related to the investigations on ZnS quantum dots (or nanocrystals) doped with such ions [4, 5]. EPR spectroscopy plays a major role due to both high absolute sensitivity and the ability to detect small changes in the local crystal field, resulting from different localization of the paramagnetic impurity ions and/or changes in the configuration and nature of the neighbouring ligands [6]. The determination of such configuration variations and the separation of the bulk and surface properties from the quantum confinement effects in nanocrystalline ZnS require accurate reference EPR spectrum parameter values for the bulk material. However, one finds out that even in the case of Mn^{2+} ions, the most investigated impurity in nanocrystalline ZnS with cubic structure, the various sets of spin Hamiltonian (SH) parameters for the bulk crystals reported in the literature [7–12] exhibit rather large variations, comparable to the variations in the corresponding values for nanocrystalline ZnS [13–18]. Thus, the interpretation of the EPR spectra becomes questionable, as the variations in the SH parameters attributed to changes in the local crystal field due to different localizations of the Mn^{2+} ions in the ZnS nanostructures might be just the result of experimental errors.

Besides a more accurate set of reference SH parameters for the cubic ZnS crystals, further substantial advances in understanding the properties of Mn^{2+} ions in ZnS nanocrystals are conditional on a higher accuracy in determining the SH parameters from the observed spectra, including the zero field splitting parameters (ZFS). Such accuracy cannot be achieved without including both forbidden hyperfine transitions and

line broadening mechanisms in the EPR spectra line shape simulations used in determining the SH parameters for paramagnetic ions in nanomaterials. The corresponding reference information for Mn^{2+} ions in bulk crystalline ZnS is not available in the scientific literature.

The present research is intended to fill up this informational gap, by reporting the results of a detailed X (9.8 GHz)-band EPR investigation of the substitutional Mn^{2+} ions in well oriented ZnS single crystals with pure cubic structure. The analysis of the experimental data, using computer programs for the analysis and simulation of the EPR spectra based on straightforward diagonalization of the spin Hamiltonian energy matrix, has resulted in highly accurate spin Hamiltonian parameters describing the observed transition fields within the experimental error of 0.01 mT.

The observation, for the first time in this crystal lattice host, of the central hyperfine forbidden transitions, offers experimental support for an accurate analysis of their positions and intensities as a function of the orientation. We have also performed a quantitative analysis of the line width variation of the fine structure components as a function of the rotation angle in a (110) plane, as well as the simulation of the spectrum along the $\langle 001 \rangle$ direction by including crystal field parameter fluctuations. This analysis gives, for the first time, an insight into the line broadening mechanisms acting on the Mn^{2+} ions in the bulk crystalline ZnS.

The present results offer a basis for an improved analysis of the EPR spectra of Mn^{2+} ions in ZnS quantum dots/nanocrystals, which could lead to a better understanding of their local atomic and quantum confinement related properties.

2. Experimental details

The ZnS single crystals employed in the present investigation have been grown by the gradient technique in melted $PbCl_2$ at temperatures where the cubic phase is stable. Fused silica (Vitreosil grade) ampoules were filled with reagent grade $PbCl_2$ (Reactivul) and ZnS (Balzers) in a 2:1 molar ratio, dried under vacuum and sealed off. Mn^{2+} doped ZnS single crystals were grown by adding 0.5 mol% of $MnCl_2$ to the starting materials. The sealed ampoules were afterwards lowered into a temperature controlled two zone furnace with a temperature gradient of 5 °C cm^{-1}. The recrystallization and growth of the ZnS crystals took place at the bottom of the ampoule, which was kept at $T = 575$ °C as compared to 600 °C in the upper part. Transparent, plate-like single crystals with well developed facets, of up to several millimetres on the largest sides, exhibiting a pure cubic ZnS structure and a very low concentration of extended defects have been obtained [19]. The single crystals could be relatively easily cleaved in the (110) planes resulting in shiny, mirror-like surfaces. The undoped single crystals exhibited a slightly yellow-amber tint, attributed to the presence of traces of copper (<10 ppm) from the starting ZnS powder [20]. The manganese doped ZnS single crystals exhibited a slightly greenish colouration. The EPR measurements have been performed at room temperature (RT) on a Varian E-line spectrometer recently upgraded with a Bruker digital EMX-plus console connected to a high sensitivity Premium X microwave bridge and cavity. The V7000 series 12″ electromagnet was driven by a specially adapted Hall controlled ultra-stable power supply, also from Bruker. The microwave frequency and the magnetic field were measured with an accuracy of 10^{-6} with the built-in frequency counter and NMR Teslameter (model ER 036TM), respectively. The absolute sensitivity of the spectrometer was found to be better than 1.6×10^9 spins/0.1 mT (Varian type weak pitch). The magnetic field at the sample has been calibrated with reference to DPPH (α, α'-diphenyl-β-picryl hydrazil) and a polycrystalline (CVD-chemical vapour deposition grown) diamond sample containing paramagnetic N^0 centres which exhibit a central narrow EPR line at $g = 2.0024$ [21]. The magnetic field calibration was also tested by setting the magnetic field at a fixed value and determining with the NMR Teslameter the magnetic field gradient between its normal position, during the EPR measurements, next to the microwave cavity, and at the sample position, in the magnet centre. The two magnetic field calibration tests were found to agree.

The determination of the spin Hamiltonian parameters has been performed with the computer program EPRNMR v. 6.4 (Department of Chemistry, University of Saskatchewan, Canada). For the line shape simulations we employed the SIM specialized program [22, 23], developed by H Weihe at the Chemistry Department of the University of Copenhagen, Denmark.

The investigated ZnS single crystal samples were glued to the flat polished side of a 4 mm diameter pure fused silica (Suprasil grade) rod, with a $\langle 110 \rangle$ direction parallel to the rotation axis and perpendicular to the magnetic field. The alignment was done optically, with reference to the natural facets and/or cleavage planes and resulting edges. It was further improved with respect to the magnetic field by tilting the microwave cavity with the crystal sample and maximizing the fine structure splitting for the $H \| \langle 001 \rangle$ orientation. The final alignment of the crystal axes with respect to the magnetic field was estimated to be within a $\pm 0.25°$ accuracy. To avoid microwave saturation effects the EPR spectra were recorded at microwave power levels of $P < 5 \times 10^{-4}$ and 10^{-4} W in the case of the manganese doped and undoped crystals, respectively.

3. Results

Similar anisotropic EPR spectra due to Mn^{2+} ions at sites with cubic symmetry, but with different intensities and line widths, were observed in both undoped and manganese doped ZnS single crystals (figure 1). The spectra consist of six sets of five fine structure transitions, best resolved for the $H \| \langle 001 \rangle$ orientation. The spectrum was described in [7] by considering the hyperfine parameter $A > 0$. Later on, Watkins [8] showed from low temperature EPR measurements that $A < 0$. The spectra presented in figure 1 are described with the correct quantum number notation of the observed transitions. Only the upper M value of each fine structure $M \leftrightarrow M - 1$ transition is mentioned.

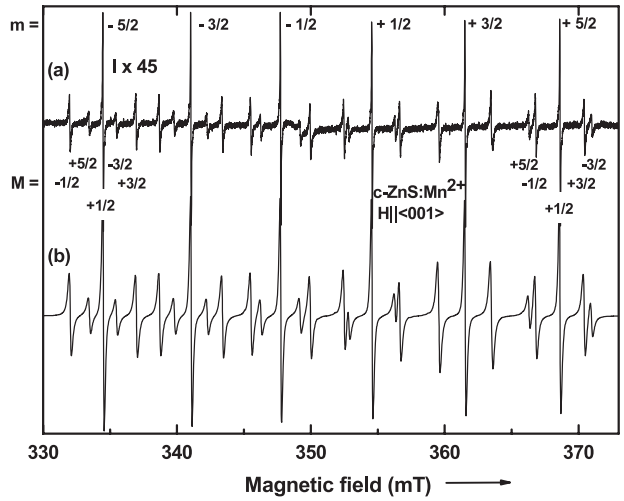

Figure 1. EPR spectra recorded at RT for the magnetic field parallel to a ⟨001⟩ crystal axis, at 9856.5 MHz, for (a) undoped and (b) Mn^{2+} doped ZnS single crystals, respectively. For clarity only the quantum numbers associated with the fine structure component lines of the $m = -5/2$ and $+5/2$ hyperfine transitions are shown in the upper spectrum of the undoped crystal, which is recorded with a gain 45 times larger than the spectrum of the doped crystal.

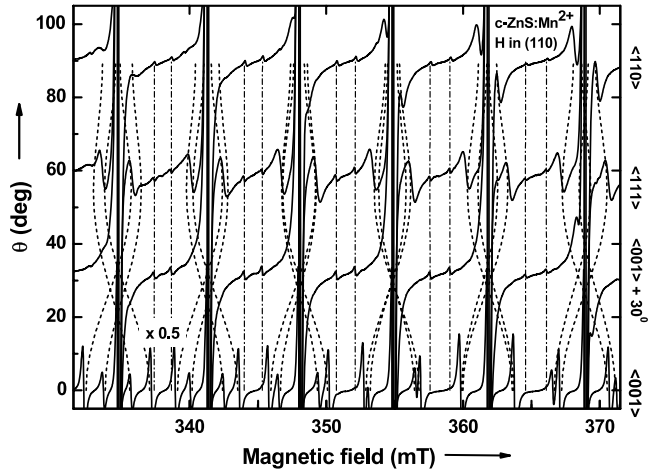

Figure 2. The angular dependence of the EPR transitions of the Mn^{2+} ions in cubic ZnS single crystals on the rotation of the magnetic field away from ⟨001⟩ in a (110) plane, at 9865.35 MHz. Dashed lines correspond to allowed transitions and dot and dashed lines to the hyperfine forbidden $\Delta m = \pm 1$ transitions. The angular variation is superimposed on the EPR spectra, which were recorded for particular orientations of the magnetic field, at high gains, in order to make visible the forbidden hyperfine transitions. For clarity the $H \| \langle 001 \rangle$ spectrum is shown at 1/2 of the gain used for the other spectra.

The EPR spectra observed in the undoped ZnS crystals are due to Mn^{2+} impurities present in the starting materials, estimated to be less than 0.1 ppm in concentration. Comparing the intensity of the EPR spectra, defined as the double integral of the recorded derivative absorption signal, one estimates the concentration of the Mn^{2+} ions in the doped ZnS single crystals to be about three orders of magnitude higher than in the undoped crystals. No EPR transitions that could be attributed to other paramagnetic species have been detected in the investigated ZnS crystals. Although copper is known to exist in these crystals [20], the absence of any associated EPR spectrum is attributed to its presence either in a non-paramagnetic Cu^{+} ($3d^{10}$) valence state, or, in the case of a Cu^{2+} ($3d^{9}$) state, to temperature-induced line broadening effects.

3.1. Determination of the spin Hamiltonian parameters

The angular dependence of the EPR spectra obtained by rotating the magnetic field in a (110) plane (figure 2) shows the characteristic pattern of the Mn^{2+} ions in a cubic crystal field [7, 10]. The EPR line positions are determined by diagonalization of the following spin Hamiltonian (SH), which describes the energy levels of a $3d^5$ (^6S) ground state in a cubic crystal field [24]:

$$H = \mu_B \vec{S}\hat{g}\vec{H} + \frac{a}{6}[(S_x^4 + S_y^4 + S_z^4) - \tfrac{1}{5}S(S+1)(3S^2+3S-1)] + \vec{S}\hat{A}\vec{I} - g_n\mu_n\vec{H}\vec{I}. \quad (1)$$

Here (x, y, z) are the main cubic axes and $S = I = 5/2$.

In early works [7–10], the SH parameters were determined in an approximate manner by expressing them as a function of the transition fields and microwave frequency, using perturbation formula to the second order to express the energy levels as a function of the magnetic field and SH parameters and resolving the corresponding equations. In our case, the SH parameters were determined with the aid of the EPRNMR software by direct numerical diagonalization of (1) and fitting the experimental lines of the allowed transitions recorded with the magnetic field along the main ⟨001⟩, ⟨111⟩ and ⟨110⟩ orientations. The resulting values and estimated accuracy are presented in table 1, together with the early reported values. One should mention that just by fitting the 30 allowed transition fields observed for the $H \| \langle 001 \rangle$ orientation we already obtained a set of SH parameter values very close to those reported in table 1, as expected for a well oriented sample. The accuracy of the resulting SH parameters has been further checked by comparing the calculated and experimental line positions determined from the spectra recorded with the magnetic field rotated in steps of 5° from ⟨001⟩ in a (110) plane. For the well resolved lines the fitting was within experimental errors of ±0.01 mT.

3.2. Line broadening effects

A simple evaluation of the expected intensity of the five fine structure components based on calculation of the transition probabilities for $H \| \langle 001 \rangle$ results in a ratio of 8:5:9:5:8 for each hyperfine transition [7]. The ratio of the derivative peak-to-peak amplitude, or simply intensity, of the experimental EPR line components presented in figure 1 is approximately 5:3:9:3:5 in the case of the undoped ZnS sample and 7:4:9:4:7 in the case of the doped sample. The observed intensity ratio variation is attributed to the inhomogeneous line broadening, resulting in an increased line width for the anisotropic fine structure components. Indeed, the ratio of the integrated intensity of the fine structure component

Table 1. The SH parameter values and their estimated accuracy for the Mn^{2+} impurity ions in cubic ZnS crystals reported in the literature, as well as the corresponding values determined in this investigation.

c-ZnS: Mn^{2+} crystals	T (K)	g	a (10^{-4} cm^{-1})	A (10^{-4} cm^{-1})	Observations
Natural blende[a]	RT	2.0025 ± 0.0002	7.76 ± 0.01	-63.94 ± 0.1	Sign of A according to [8]
Natural blende[b]	RT	2.0021	7.97	-63.73	Crystals also investigated in [7]
Grown by transport in vapours[c]	RT	2.0024 ± 0.0003	7.87 ± 0.06	-64.0 ± 0.1	Small axial component included for description of the EPR spectra
	77	2.0022 ± 0.0003	7.94 ± 0.06	-64.5 ± 0.1	
Vacuum grown at 700 °C[d]	4.2		8.17(9)	-64.657	ENDOR investigation at 35 GHz. An axial ZFS component and the nuclear quadrupole term were included in the SH
Crystalline powders[e]	RT	2.0022		64.0	Containing non-cubic crystalline phases
Grown from $PbCl_2$ melt at 725 °C[f]	RT	$2.00225 \pm 0.000\,06$	7.987 ± 0.008	-63.88 ± 0.02	Pure cubic crystalline phase

[a] Reference [7, 8]; [b] Reference [9]; [c] Reference [10]; [d] Reference [11]; [e] Reference [12]; [f] This work.

lines is close to the theoretical ratio for both types of ZnS crystals. The line broadening, which has been observed in the EPR spectra of many other high quality crystals doped with paramagnetic ions, such as Mn^{2+} doped tungstate or calcite single crystals [25–28], was attributed to the presence of random strains, electric fields and other perturbations from extended and point defects in the crystal lattice [29].

The quantitative description of the EPR line broadening is based on the assumption that the perturbations induced by the various lattice defects result in variations in the local crystal field at the paramagnetic ion described as fluctuations of the zero field splitting (ZFS) parameters [30]. Such fluctuations determine an increased line width for the fine structure component lines, which is also dependent on the orientation in the magnetic field.

Another source of line broadening is the magnetic dipolar interaction between the impurity ions, which is concentration dependent. It explains why in our manganese doped ZnS crystals the EPR spectra line width ΔH is ~2.5 times larger than the undoped ZnS crystals (e.g. for the $M = +1/2 \leftrightarrow -1/2$ allowed transitions at $H \| \langle 001 \rangle$, $\Delta H = 0.035$ mT for the undoped ZnS crystal, while for the manganese doped crystal $\Delta H = 0.097$ mT). To avoid the perturbing magnetic dipolar interaction broadening effects, we decided to investigate the undoped ZnS crystals, where the Mn^{2+} concentration is sufficiently low for the paramagnetic ions to be well separated in the crystal lattice and the dipolar line broadening effects to be negligible. The line shape analysis has been performed for the $H \| \langle 001 \rangle$ spectrum, which exhibits the best resolved structure. As shown in figure 3, in order to obtain a good simulation/fitting of the experimental spectrum we had to consider small fluctuations not only in the fourth order crystal field parameter a, but also to include small variations around the zero value in the axial field parameter D. The best simulation was obtained for a Gaussian distribution of the a parameter values around the mean value given in table 1 with standard deviation $\sigma(a) = 2.4 \times 10^{-5}$ cm^{-1}, and a Gaussian distribution around the $D = 0$ value with standard deviation $\sigma(D) = 1.3 \times 10^{-5}$ cm^{-1}. Figure 4 presents a detailed view of the $m = -5/2$ fine structure lines, which allows a better

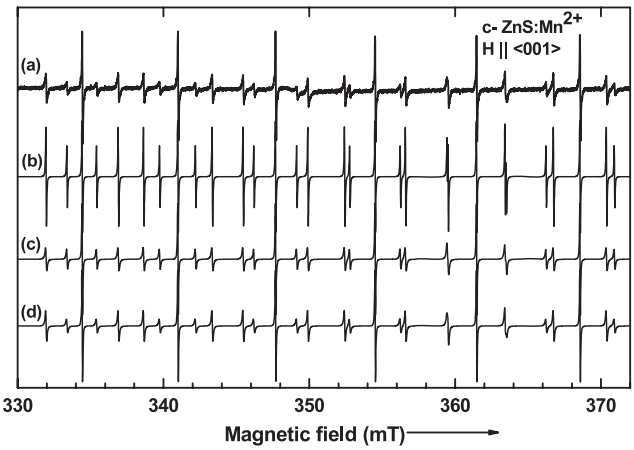

Figure 3. (a) The experimental EPR spectrum of the Mn^{2+} ions in undoped ZnS crystals at 9856.6 MHz for $H \| \langle 001 \rangle$ compared to: (b) the calculated/simulated line shape with the SH parameters given in table 1, for a Lorentzian line shape, without considering line broadening effects; (c) a Gaussian distribution of the cubic ZFS parameter a with the standard deviation $\sigma(a) = 2.4 \times 10^{-5}$ cm^{-1} and (d) after including a Gaussian distribution of the axial ZFS parameter D with standard deviation $\sigma(D) = 1.3 \times 10^{-5}$ cm^{-1} as well.

observation of the changes induced in the line shape by the line broadening mechanisms.

We have also investigated the angular variation in the (110) plane of the peak-to-peak line width of the $M = +1/2 \leftrightarrow +3/2$, $m = -5/2$ and $M = -3/2 \leftrightarrow -5/2$, $m = +5/2$ fine structure transitions, which were better resolved in a larger angular range. It has been shown by Barberis *et al* [28] that the angular dependence of the line width is directly correlated to the symmetry of the source of the broadening, which can be the same as or higher than the point symmetry at the paramagnetic ion, therefore being cubic in our case. Indeed, as shown in figure 5, the experimental points could be fitted with an angular variation corresponding to cubic symmetry [25, 28]:

$$\Delta H = A_1 + A_2 \cos^4\theta + A_3 \cos^2\theta + A_4 \sin^4\theta \cos 4\phi \quad (2)$$

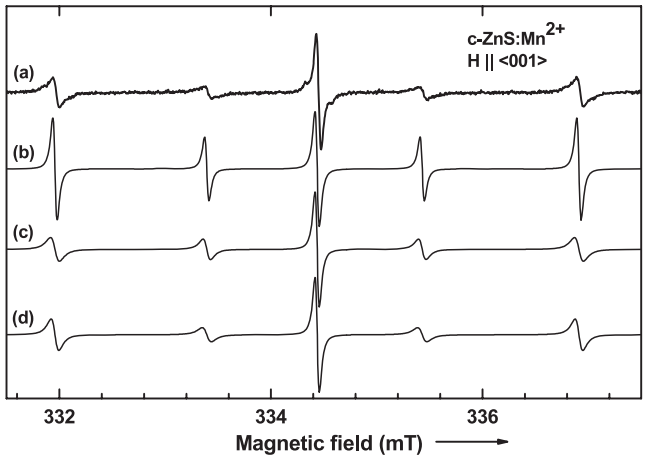

Figure 4. Detailed view of figure 3, presenting the experimental and simulated line shape of the low field fine structure component lines of the $m = -5/2$ hyperfine transition.

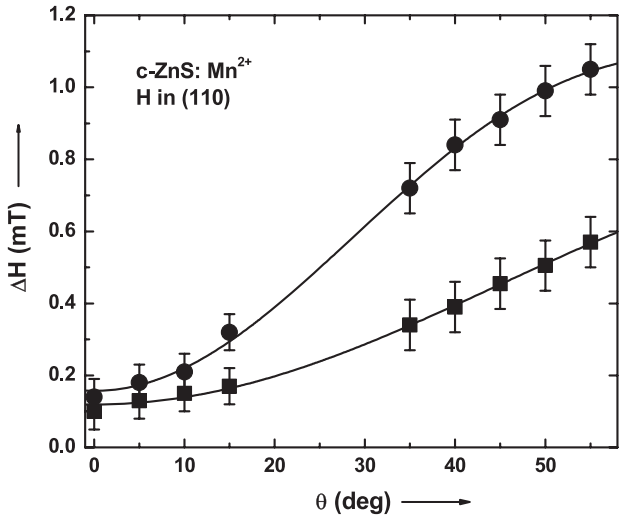

Figure 5. The angular variation in the (110) plane of the line width of the fine structure transitions $M = +3/2 \leftrightarrow +1/2$, $m = -5/2$ (filled squares) and $M = -3/2 \leftrightarrow -5/2$, $m = +5/2$ (filled circles), for an unintentionally Mn^{2+} doped ZnS single crystal. The calculated values are represented by continuous lines.

where $\phi = 45°$ in the (110) plane and $A_1 = (0.20 \pm 0.04)$ mT; $A_2 = -(0.59 \pm 0.09)$ mT, $A_3 = (0.50 \pm 0.12)$ mT, $A_4 = -(0.58 \pm 0.4)$ mT for the $M = +1/2 \leftrightarrow +3/2$, $m = -5/2$ transition and $A_1 = (0.42 \pm 0.06)$ mT; $A_2 = -(1.86 \pm 0.13)$ mT; $A_3 = (1.60 \pm 0.18)$ mT; $A_4 = -(0.66 \pm 0.06)$ mT for the $M = -3/2 \leftrightarrow -5/2$, $m = +5/2$ transition.

One should also mention that a similar experimental line width angular variation of the fine structure transitions was reported in [10], although the reported line width of 0.05 mT for the $M = +1/2 \leftrightarrow -1/2$ allowed transitions at $H \| \langle 001 \rangle$ is slightly larger than in our case. This could be due to either a lower quality of the investigated ZnS crystals or to a higher concentration of Mn^{2+} impurity ions.

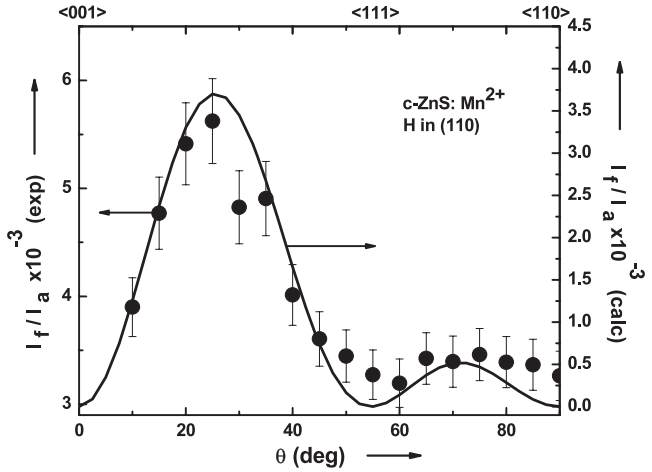

Figure 6. Experimental (dots) and calculated (continuous line) angular variation of the ratio of the average intensity of the hyperfine forbidden transitions $M = +1/2 \leftrightarrow -1/2$, $m = +1/2 \leftrightarrow -1/2$ and $M = +1/2 \leftrightarrow -1/2$, $m = -1/2 \leftrightarrow +1/2$ doublet to the corresponding intensity of the neighbouring allowed $M = +1/2 \leftrightarrow -1/2$, $m = +1/2$ and $M = +1/2 \leftrightarrow -1/2$, $m = -1/2$ transitions, for rotation of the magnetic field in a (110) plane. Measuring frequency is 9865 MHz.

3.3. The forbidden hyperfine transitions

The so-called forbidden hyperfine transitions, in which both electron and nuclear magnetic quantum numbers are changing ($\Delta M = \pm 1$, $\Delta m = \pm 1$), are expected to occur between the intense allowed hyperfine ($\Delta M = \pm 1$, $\Delta m = 0$) transitions, for orientations away from the twofold or higher symmetry main crystal axes [31]. Such transitions have been previously investigated in cubic single crystals with rock salt (MgO) and blende (ZnSe) structure doped with Mn^{2+} ions [32, 33]. It has been shown that, although their position is isotropic, their intensity is anisotropic. The presence in cubic ZnS crystals of hyperfine forbidden transitions has been briefly mentioned in [34]. However, the reported anisotropy in their position strongly suggests that the observed spectrum originated in fact from Mn^{2+} ions in non-cubic crystalline phases/polytypes.

As shown in figure 2, we were able to observe clearly in our manganese doped cubic ZnS single crystals, for all orientations in the (110) plane, including the $H \| \langle 001 \rangle$ orientation, the central $M = +1/2 \leftrightarrow -1/2$, $\Delta m = \pm 1$ hyperfine forbidden transitions. In the undoped crystals, due to the lower intensity of the whole spectrum, these transitions could be seen only after multiple spectrum accumulations in the highest sensitivity conditions. In both cases, their isotropic positions could be predicted within the experimental errors of 0.01 mT with the same SH parameters given in table 1. This is illustrated in figure 2 for the spectra recorded along the three main crystal axes.

We have also investigated the variation in the intensity ratio I_f/I_a between the central forbidden and allowed transitions, respectively. According to early analytical calculations it varies as $\sin^2(4\theta)$, being zero for the main $H \| \langle 001 \rangle$ and $H \| \langle 110 \rangle$ orientations [32, 33]. As shown in figure 6 by a continuous line, the angular variation of the

I_f/I_a ratio for the magnetic field rotated in a (110) plane, calculated by direct diagonalization of the energy matrix with both employed computer programs, reproduces quite well the $\sin^2(4\theta)$ dependence. However, the calculated and experimental values, of which the last could not be accurately determined within $\pm 10^\circ$ from $\langle 001\rangle$ due to the overlap with the tails of the intense neighbouring fine structure component lines, compare reasonably well only if one subtracts from the experimental values a constant contribution of 0.003, which is about 50% of the maximum experimental I_f/I_a ratio. A similar doubling of the I_f/I_a ratio as compared to the calculated values and its non-zero value for the main crystalline directions was also reported in the case of the ZnSe lattice host and attributed to a large crystal misorientation of about 2° [33]. This is not the case in our investigation and another explanation should be found.

4. Discussion

The differences in the SH parameter values of the Mn^{2+} ions in the cubic ZnS bulk crystals reported by different authors can be due to several factors: instrumental errors in determining the EPR line positions, a lower precision in orienting the crystal samples in the magnetic field, or the approximate formula for the energy levels used in determining the SH parameters from the experimental data. The localization of the Mn^{2+} ions at extended defects, mainly stacking faults and inclusions of non-cubic crystal phases/polytypes may explain why, in certain cases [10, 11], small axial terms also had to be included in the SH in order to describe accurately the observed spectra.

The SH parameter values reported in the present research, almost one order of magnitude more accurate than the previous reported values (table 1), offer the possibility to find out whether the observed differences were due to the approximate energy levels as a function of the SH parameter formulae earlier employed and/or to the less accurate orientation of the samples in the magnetic field. To find out the answer we determined the SH parameters from our experimental data with the approximate formulae given in [7]. Thus, from the separation of the central ($M = +1/2 \leftrightarrow -1/2$, $m = -1/2$) and ($M = +1/2 \leftrightarrow -1/2$, $m = +1/2$) transitions one finds $A = -6.825$ mT (-63.80×10^{-4} cm^{-1}). Also, from the distances $5a - 2A^2/H_0 = 2.017$ mT and $4a + 4A^2/H_0 = 0.4946$ mT, between the pairs of fine structure transitions ($M = +1/2 \leftrightarrow -1/2$ and $M = +3/2 \leftrightarrow +1/2$) and ($M = +5/2 \leftrightarrow +3/2$ and $M = -3/2 \leftrightarrow -5/2$), respectively, for $m = -5/2$ we find that $a = 0.851$ mT (7.95×10^{-4} cm^{-1}). Finally, from the position of the $M = +1/2 \leftrightarrow -1/2$, $m = +1/2$ transition described by the resonance field $H = H_0 - A/2 - A^2(17/2) = 354.95$ mT, one obtains $H_0 = 352.09$ mT and $g = 2.0023$. A comparison with the values given in table 1 shows that the values of the SH parameters obtained by approximate calculations are closer to the values reported in [9] and to the exact values we obtained by numerical diagonalization of the SH (formula (1)), as compared to the other sets of reported SH parameters. This result suggests that the sample misalignment is the main source of errors. Indeed, the variation is larger in the case of the cubic crystal field parameter a, its determination being more sensitive to the misalignment of the sample in the magnetic field, especially for $H \| \langle 001\rangle$.

In the case of the central forbidden hyperfine transitions, their positions were found to be isotropic and could be predicted with our SH parameters reported in table 1 within 0.01 mT accuracy. These transitions were previously reported in isostructural ZnSe crystals [33], their positions being predicted only within 0.06 mT accuracy by using the approximate formulae.

Contrary to calculations, we found out, as previously reported in other cubic crystals [32, 33], that the experimental intensity ratio I_f/I_a is different from zero even for the magnetic field along the main crystal axes. The effect is due to a relatively large additional isotropic contribution, comparable to the largest theoretical value. The relative magnitude of the isotropic contribution is even larger if one considers the phonon-induced correction, which was shown to decrease the I_f/I_a ratio with the temperature increase [34]. Thus, in the case of the Mn^{2+} ions in cubic MgO crystals the experimentally observed decrease at RT was about 5% of the zero temperature value. The origin of the isotropic contribution to the intensity of the forbidden transitions is not yet clear. The effect of the magnetic dipole–dipole interaction between the paramagnetic Mn^{2+} ions can be neglected. Indeed, our experimental determinations of the I_f/I_a ratio for orientations of the magnetic field in a (110) plane, around $\langle 001\rangle + 30^\circ$ orientation, have resulted in the same values for the undoped and Mn^{2+} doped ZnS single crystals.

We have also shown that the observed line broadening of the fine structure transitions can be explained by considering small fluctuations in both fourth order crystal field parameter a and small variations around the zero value in the axial field parameter D, which are present even in the highest quality cubic ZnS single crystals employed in our investigation. The line broadening also explains the absence in the observed EPR spectrum of the Mn^{2+} doped ZnS single crystals of the non-central $M = \pm 5/2 \leftrightarrow \pm 3/2$, $\Delta m = \pm 1$ and $M = \pm 3/2 \leftrightarrow \pm 1/2$, $\Delta m = \pm 1$ hyperfine forbidden transitions, which, according to our computations, are comparable in intensity with the corresponding central transitions.

One should also mention that the non-zero local fluctuating axial crystal field, responsible for the line broadening effects, could also be the source of the isotropic contribution to the I_f/I_a ratio.

It is interesting to see how the observed line broadening influences the EPR spectrum line shape of the Mn^{2+} ions in polycrystalline/nanocrystalline ZnS. Figure 7 presents a powder EPR spectrum line shape simulation with our SH parameters (table 1). The simulation, based on the EPR line width data from the ZnS single crystals with Mn^{2+} impurity concentration (~500 ppm) comparable to that reported in nanocrystalline ZnS exhibiting well resolved EPR spectra [14–18], has been performed both in the absence of line broadening, considering a constant $\Delta H = 0.097$ mT line width (figure 7(a)) and by including the line broadening effect, described in these samples by the characteristic parameters $\sigma(D) = 3 \times 10^{-4}$ cm^{-1} and $\sigma(a) = 3.2 \times 10^{-4}$ cm^{-1}

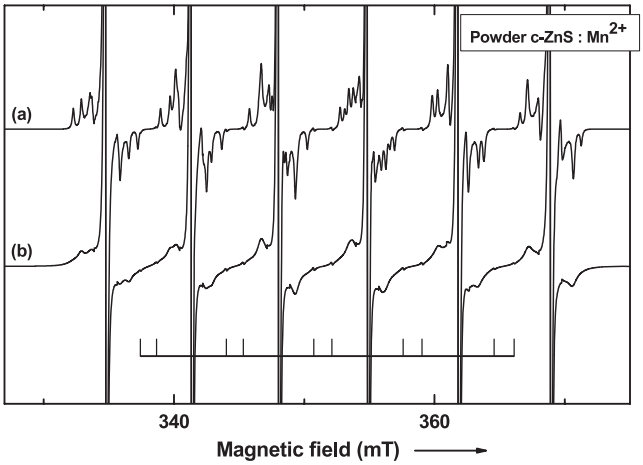

Figure 7. Simulated line shape of the EPR spectrum of Mn^{2+} ions in polycrystalline cubic ZnS computed with the SH parameters determined in the present research (table 1) at 9865 MHz, considering as line width: (a) a constant 0.097 mT value and (b) including the line broadening effects observed in the case of Mn^{2+} doped ZnS single crystals. The central hyperfine forbidden transitions are indicated by the vertical bars at the bottom of the figure.

(figure 7(b)). In agreement with our experimental results, the intensity of the central hyperfine forbidden transitions was taken as twice the calculated value, resulting in a $I_f/I_a \sim 10^{-3}$ ratio. Comparing the two powder spectra simulations one concludes that even such small line broadening parameters, characteristic for high quality ZnS single crystals, can strongly influence the shape of the powder EPR spectrum by practically burying the fine structure lines into the broadened tails of the six central hyperfine transitions. Such effects are expected to play an increased role in the case of the nanocrystalline ZnS, where the degree of crystalline lattice disorder is much larger, resulting in major difficulties in the determination of the ZFS parameters. Our results also show that the central hyperfine forbidden transitions are very likely to appear in the powder-like EPR spectra of Mn^{2+} doped nanocrystalline cubic ZnS. Therefore, their presence does not mean that non-cubic crystal field components are necessarily present at the Mn^{2+} impurity ion site, as assumed in some cases [17, 35].

Acknowledgments

The present research has been performed in the framework of the projects CEEX No. 33/2006 and PN-II-ID-PCE No. 828/2008 of the Romanian Ministry of Education and Research. We thank D Zernescu for expert technical assistance.

References

[1] Curie D and Prener J S 1967 *Physics and Chemistry of II–VI Compounds* ed M Aven and J S Prener (Amsterdam: North-Holland) chapter 9, p 440
[2] Godlewski M and Leskela M 1994 *CRC Crit. Rev. Solid State Mater. Sci.* **19** 199
[3] Kikoin K A and Fleurov V N 1994 *Transition Metal Impurities in Semiconductors* (Singapore: World Scientific)
[4] Zheng W C and Wu X X 2005 *J. Phys. D: Appl. Phys.* **38** 4157–59
[5] Hu H and Zhang W 2006 *Opt. Mater.* **28** 536–50
[6] Erwin S C, Zu L, Haftel M I, Efros A L, Kennedy Th A and Norris D J 2005 *Nature* **436** 91–4
[7] Matarrese L M and Kikuchi C 1956 *J. Phys. Chem. Solids* **1** 117–27
[8] Watkins G D 1958 *Phys. Rev.* **110** 986
[9] Walsh W M Jr 1961 *Phys. Rev.* **122** 762–7
[10] Schneider J, Sircar S R and Rauber A 1963 *Z. Naturf.* a **18** 980–93
[11] de Beer R, Biesboer F and van Veen G 1977 *Z. Naturf.* a **32** 724–30
[12] Kreissl J 1968 *Phys. Status Solidi* a **97** 191
[13] Kennedy T A, Glaser E R, Klein P B and Bhargava R N 1995 *Phys. Rev.* **52** R14356
[14] Borse P H, Srinivasa D, Shinde R F, Date S K, Vogel W and Kulkarni S K 1999 *Phys. Rev.* B **60** 8659
[15] Liu J, Liu C, Zheng Y, Li D, Xu W and Yu J 1999 *J. Phys.: Condens. Matter* **11** 5377
[16] Igarashi T, Ihara M, Kusunoi T, Ohno K, Isobe T and Senna M 2001 *J. Nanopart. Res.* **3** 51
[17] Gonzalez Beermann P A, McGarvey B R, Muralidharan S and Sung R C W 2004 *Chem. Mater.* **16** 915
[18] Gonzalez Beermann P A, McGarvey B R, Skadtchenko B O, Muralidharan S and Sung R C W 2006 *J. Nanopart. Res.* **8** 235
[19] Nistor L C, Nistor S V and Toacsan M I 1980 *J. Cryst. Growth* **50** 557
[20] Nistor S V and Toacsan M I 1980 *Rev. Roum. Phys.* **25** 707
[21] Vlasov I I, Ralchenko V G, Komich A V, Nistor S V, Schoemaker D and Khmelnitskii R A 2000 *Phys. Status Solidi* a **181** 83–90
[22] Glerup J and Weihe H 1991 *Acta Chem. Scand.* **45** 444
[23] Jacobsen C J H, Pedersen E, Villadsen J and Weihe H 1993 *Inorg. Chem.* **32** 1216
[24] Abragam A and Bleaney B 1970 *Electron Paramagnetic Resonance of Transition Ions* (Oxford: Clarendon)
[25] Barberis G E and Calvo R 1973 *Solid State Commun.* **12** 963
[26] Nistor S V, Stefan M, Goovaerts E, Nikl M and Bohachek P 2004 *Radiat. Meas.* **38** 655
[27] Marshall S A and Reinberg A R 1963 *Phys. Rev.* **132** 134
[28] Barberis G E, Calvo R, Maldonado H G and Zarate C E 1975 *Phys. Rev.* B **12** 853
[29] Stoneham A M 1969 *Rev. Mod. Phys.* **41** 82
[30] Pilbrow J R 1990 *Transition Ion Electron Paramagnetic Resonance* (Oxford: Clarendon)
[31] Bleaney B and Rubins R S 1961 *Proc. Phys. Soc.* **77** 103
[32] Drumheller J E and Rubins R S 1964 *Phys. Rev.* **133** A1099
[33] Cavenett B S 1964 *Proc. Phys. Soc.* **84** 1
[34] Srivastava K N and Drumheller J E 1969 *Phys. Rev.* **184** 271
[35] Cunio G, Esnouf S, Gacoin T and Boilot J-P 1996 *J. Phys. Chem.* **100** 20021